World Journal of Engineering and Technology, 2017, 5, 134-151
http://www.scirp.org/journal/wjet
ISSN Online: 2331-4249
ISSN Print: 2331-4222

A Novel Blood Coagulation Measuring Method Based on the Viscoelasticity of Non-Newtonian Fluid

Jiahua Kou, Yuhe Li, Pengyan Yang, Jintong Zhang

The State Key Laboratory of Precision Measuring Technology and Instruments, Department of Precision Instrument, Tsinghua University, Beijing, China
Email: kjh15@mails.tsinghua.edu.cn, liyuhe@mail.tsinghua.edu.cn

How to cite this paper: Kou, J.H., Li, Y.H., Yang, P.Y. and Zhang, J.T. (2017) A Novel Blood Coagulation Measuring Method Based on the Viscoelasticity of Non-Newtonian Fluid. *World Journal of Engineering and Technology*, **5**, 134-151.
https://doi.org/10.4236/wjet.2017.54B015

Received: September 15, 2017
Accepted: October 9, 2017
Published: October 12, 2017

Abstract

There are complex and perfect coagulation, anticoagulation and fibrinolysis systems in the human body and their fine regulatory mechanisms. Once the coagulation system and its regulatory mechanisms are destroyed, bleeding or thrombosis will occur very soon. In the blood coagulation, the blood viscoelasticity changes. Therefore, the thrombus elasticity measurement technology can be used to continuously monitor the changing blood viscoelasticity in order to study the process of coagulation. The results of the interaction among the various components of the blood can be obtained from coagulation to fibrinolysis by bedside detection. The traditional electromagnetic induction sensors, based on conventional coil inductance, are manufactured complexly, high cost and non-linear. Therefore, this paper proposes a non-Newtonian fluid viscoelasticity measurement method based on the piezoelectric effect. We use the piezoelectric bimorphs with the diameter of 21 mm and the total thickness of 0.38 mm and DSM coupling probes with the length of 3 mm, 5 mm and 7 mm to design the piezoelectric bimorphs driver. The viscoelasticity of different non-Newtonian fluids is tested. The vibration amplitudes of the piezoelectric bimorphs and liquid surfaces range from 0.43 μm to 3.52 μm. Consequently, the feasibility of *in vitro* detection of thrombus is confirmed in principle and the above scheme is validated theoretically and experimentally, which provides the basis for the measurement of blood viscoelasticity, the *in vitro* detection of thrombus and the manufacture of blood coagulation instrument.

Keywords

Blood Coagulation, Viscoelasticity, Non-Newtonian Fluid, Embedded System

1. Introduction

There exist complex and perfect coagulation, anticoagulation, and fibrinolysis systems in the human bodies and their fine regulatory mechanisms. Blood in veins, arteries and capillaries is neither bleeding from vessel walls nor thrombotic in normal physiological conditions. However, once the above system and its regulatory mechanisms are damaged, bleeding or the formation of thrombosis will occur immediately and pose a grave threat to human bodies. Until the 19th century, bleeding time detected by the methods of "point of care testing (POCT)" was considered as a regular measure of coagulation function indicators [1]. After a long time, the blood coagulation test still required complex and delicate operation and the basic principle of blood coagulation test found in the 19th century, which referred to that biological tissue would accelerate the blood coagulation if it was contacted with glass containers [2]. Advances in the blood coagulation test technology and the discovery of coagulation cascade have contributed to the rapid development of coagulation time testing. The main test methods include prothrombin time (PT), activated partial thromboplastin time (APTT), thromboplastin time (TT), and activation of coagulation time (ACT) [3] [4]. In order to obtain a comprehensive and effective evaluation of the blood coagulation and fibrinolysis function, it is far from enough to rely on routine tests and regular indicators, especially in a large surgical procedure such as a cardiac surgery and a liver transplant. It is acknowledged that a more definite coagulation test means a higher surgical success [5]. However, it is not practical to detect each biological event in the blood coagulation and fibrinolysis process with the large number of equipment and cumbersome tests. Clinicians also need a simple and intuitionistic evaluation of the whole blood coagulation, especially in a set of POCT methods and equipment to detect blood coagulation function the perioperative period [6].

In the blood coagulation cascade, the protein, platelets, blood cells can firstly form into a three-dimensional and cross-linked network structure, and then fibrin dissolves because of the fibrinolytic enzyme. During the whole process of coagulation fibrinolysis, blood viscoelasticity changes [7]. Blood viscoelasticity detection technology is used to continuously study the changing blood viscoelasticity in the blood coagulation process. Thrombosis elastic map (TEM) obtained by data and image processing, can illustrate the whole process of the interaction of all the various components in blood coagulation and fibrinolysis. Consequently, it can allow doctors to detect the patients' blood coagulation function accurately via POCT without damage in the perioperative period and make rapid diagnosis and highly stable treatment programs. At present, kinds of blood viscoelasticity measurement are employed, including the thromboelastography (TEG), rotation thrombosis elastometer (ROTEM) and Sienco platelet function analyzer (Sonoclot). In the TEG measurement system, a probe suspended by a wire and immersed in a blood sample is applied to monitor the viscoelasticity changes in the process of blood coagulation. The shear force generated by the rotation of the blood cup can be transmitted to the probe in the blood sample, so that the amplitude of the probe and the strength of blood clots are directly related. In the ROTEM measurement, the probe is immersed in the blood sample of the cup and the probe and the cup are coupled by the blood. When the blood comes into the coagulation, the strength of the blood clot increases and the blood clot prevents the probe rotation in greater power. The kinetic changes of the probe movement recorded by the optical displacement sensor will be ROTEM and a series of test indicators. Although the TEG and ROTEM have many advantages beyond routine methods, but there are still many limitations. Firstly, *in vitro* coagulation and the actual situation of the body are different. As a result, the *in vitro* environment cannot simulate the impact exerted by the vascular endothelial cells on the vascular wall [8]. Secondly, the methods cannot distinguish different coagulation factor abnormalities, such as the MA abnormalities by TEG which means that there exist platelet or fibrinogen synthesis abnormalities without any information about the quality or quantity. Thirdly, the patients' age and gender will affect the test results [8] [9]. Moreover, the instruments are semi-automatic and the blood collection will have an impact on the results. Besides, no international uniform range of normal and the clinical decision-making threshold is not consistent. Consequently, there are the some difficulties in the clinical application. In the Sonoclot system, a disposable hollow probe connected to an ultrasonic sensor is immersed in a certain depth of the test sample (0.4 ml of blood or plasma) placed in the test cup and oscillates vertically at a certain amplitude and a frequency of 200 Hz. Due to the blood viscoelasticity, the resistance of the blood clot to the probe gradually increases. The resistance signal can be obtained from the data acquisition system and the blood clotting curve (Sonoclot) will be generated. The curve can show viscoelastic changes the in the whole process of the blood coagulation. However, Sonoclot can only detect the initial blood coagulation process and cannot detect the fibrinolytic process at present [10]. In addition, the electromagnetic drive used by Sonoclot in the vibration process is likely to lead to a large vibration amplitude in the vibration process, which will result in damage to the detection equipment. Therefore, piezoelectric materials which can generate smaller amplitude and more sensitive signal can be adopted into the detection equipment. Meanwhile, electromagnetic devices are expensive relatively and have more complicated structures. Consequently, piezoelectric bimorphs made of piezoelectric materials and copper will greatly reduce costs, while improving accuracy [11] [12].

2. System Design Schemes

The whole system shown in **Figure 1** consists of the sinusoidal signal generator, high-speed small-signal amplification module, piezoelectric bimorphs driver, DSM probes, liquid to be measured, Raspberry development board, AD-DA signal conversion circuit, display device and signal rectifier circuit. The AD620 is a low-cost, high-precision instrumentation amplifier that requires only one external resistor to

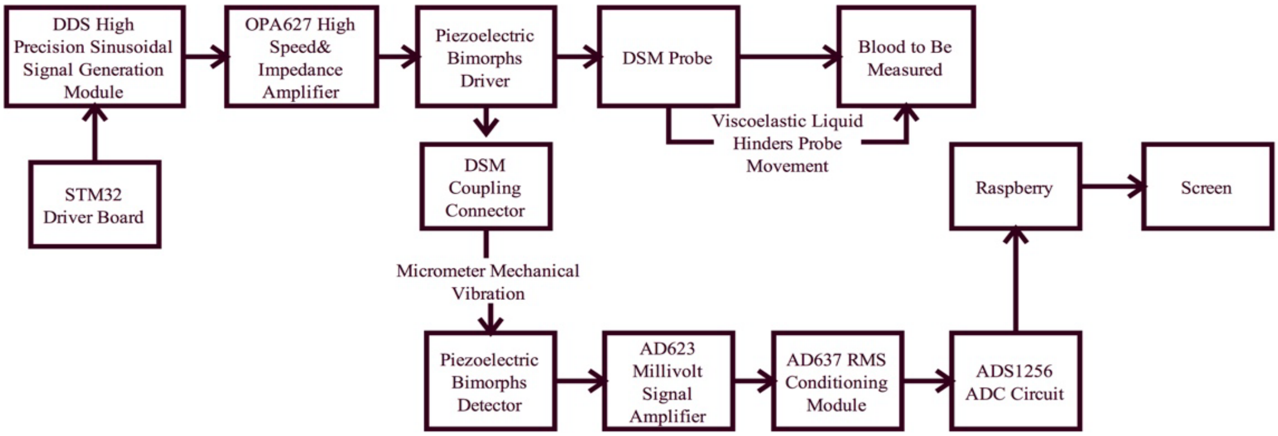

Figure 1. System design schemes.

set the gain ranging from 1 to 10,000. The OPA627 is a high-speed, high-impedance amplifier that can be used as a precision amplification module. The AD-DA conversion module features an 8-channel 24-bit high-precision ADC and a 2-channel 16-bit high-precision DAC. The embedded control system Raspberry is an ARM-based microcomputer within a SD card as the memory hard drive and considerable output interfaces. The sinusoidal signal generator DDS9959 generates a gain-adjustable sinusoidal signal to energize the lower piezoelectric bimorph. The vibration signal is then transmitted to the upper piezoelectric bimorph as the signal detection device through the coupling joint. After that, the mechanical vibration signal is converted into an electrical signal which is then transmitted to the signal rectification circuit through the signal amplification circuit. The effective value of the sinusoidal signal is obtained and sampled by the AD conversion circuit. The signal representing the non-Newtonian fluid viscoelasticity is displayed under raspberry control and is plotted as a coagulation curve to characterize the coagulation properties of the blood.

3. Theoretical Analysis

In the blood coagulation and fibrinolysis process, the blood viscoelasticity changes and the measure of the viscoelasticity is based on the change of the viscoelasticity of the blood and its dynamic measurement which can generate a continuity spectrum. The dynamic characteristics of the coagulation process can be studied through the continuity spectrum in order to detect the function of the blood coagulation.

We simplify the theory of viscoelasticity of blood and the mathematic model. After the finite element numerical simulation by COMSOL, the physical and mathematical model of the actual measurement structure is obtained. The dynamic viscoelasticity of the blood refers to the corresponding law of the mechanics of the fluid under the alternating stress or strain. Dynamic viscoelasticity measurements are usually performed at small amplitude oscillations (alternating stress or strain at small amplitude), which does not destroy the molecular chain winding structure of the blood. We can obtain the viscoelasticity of blood showing a linear viscoelastic rheological behavior. We apply a sinusoidal strain to the blood at a small amplitude:

$$\gamma(t) = \gamma_0 \sin \omega t \tag{1}$$

where γ_0 is the deformation amplitude and ω is the angular frequency. After applying the alternating strain, the stress response is also sinusoidal with the same frequency response, the stress response is:

$$\tau(t) = \tau_0 \sin(\omega t + \delta) \tag{2}$$

where there exists $0 < \delta < \dfrac{\pi}{2}$ in the viscoelastic materials, such as blood, honey and oil. The detection device consists of two piezoelectric bimorphs, a coupling joint and a probe. The edges of the two piezoelectric bimorphs are fixed. The lower one of the two piezoelectric bimorphs is an oscillating driver and the other is a vibration signal detector. When an alternating sinusoidal current signal is applied on the lower piezoelectric bimorph, the bimorph vibrates up and down with a certain amplitude to drive the coupling joint and the probe to vibrate. The coupling joint transmits the vibration to the upper piezoelectric bimorph. The deformation of the upper piezoelectric bimorph will produce an alternating electrical signal. Besides, the amplitude of the electrical signal and the amplitude of the system vibration are positively correlated.

According to the actual situation we can make the following assumptions. The center of the fixed circular area is always perpendicular to the circular plate center axis of symmetry before or after the deformation. The impact of the adhesive layer between the piezoelectric ceramic material and the electrode cannot be taken into account. The total thickness of piezoelectric ceramic, two-layer electrode, intermediate layer copper layer and adhesive layer in piezoelectric bimorphs is much smaller than that of circular piezoelectric bimorphs with a single layer structure, that is, the maximum radial dimension. Therefore, we can consider the piezoelectric bimorphs driver as a lamina. The amplitude of the piezoelectric bimorph is at the micron level, much smaller than the maximum radial dimension. Fixed constraints are at an ideal state, which can be taken as linear constraints and surface constraints, while the boundary is strictly fixed without sliding displacement.

When the piezoelectric bimorphs driver is surrounded by a fixed support, the entire piezoelectric bimorph does not have axial displacement, radial displacement and rotation along the diagonal direction of the circular plate. The edge deflection ω of the piezoelectric bimorphs is 0 and the slope of the surface of the piezoelectric bimorphs driver is 0, and the slope of the center surface is also 0 [13] [14]. Therefore, the following formula can be obtained:

$$\begin{cases} \omega|_{r=r_{copper}} = 0 \\ \dfrac{\partial \omega}{\partial r}|_{r=r_{copper}} = 0 \\ \dfrac{\partial \omega}{\partial r}|_{r=0} = 0 \end{cases} \tag{3}$$

According to the thin plate theory analysis can be obtained: when the boundary has a uniform distribution of bending moment M, we can conclude:

$$\frac{1}{r} = \frac{M}{D(1+\nu)} = \frac{\partial^2 \omega}{\partial^2 r} \tag{4}$$

where υ is the Poisson's ratio of the composite sheet, that is, the piezoelectric bimorphs, D is the bending stiffness of the composite sheet, we can conclude:

$$D = \frac{Eh^3}{12(1-\nu^2)} \tag{5}$$

The piezoelectric bimorphs driver can be viewed as a circular composite sheet applied with a quantitative load within a fixed radius [15]. In order to clearly express the quantitative relation between the applied voltage and the amplitude of the vibration, we can assume that the range of the radius is $-r_{PZT} \le r \le r_{PZT}$. According to the thin plate theory, we can conclude that the amplitude of any position relative to the support position is

$$\omega_1(r_1) = \frac{M_2}{2D_c(1+\nu_c)}(a^2 - r^2) \tag{6}$$

where D_c represents the equivalent bending stiffness of the bonded portion between the piezoelectric ceramic and the copper substrate, υ_c indicates the equivalent Poisson's ratio, M_2 represents the exact bending moment produced by the force exerted at the edge of the bonded portion of the substrate [15]. The above physical quantities can be calculated by:

$$D_c = \frac{E_c H^3}{12(1-{\nu_c}^2)} \tag{7}$$

$$\nu_c = \frac{h'_1 \nu_e E_e (1-\nu_{PZT}^2) + h'_2 \nu_{PZT} E_{PZT} (1-\nu_e^2)}{h'_1 E_e (1-\nu_{PZT}^2) + h'_2 E_{PZT} (1-\nu_e^2)} \tag{8}$$

$$E_c = h'_1 E_e + h'_2 E_{PZT} + \frac{h'_1 h'_2 E_e E_{PZT} (\nu_e - \nu_{PZT})^2}{h'_1 E_e (1-\nu_{PZT}^2) + h'_2 E_{PZT} (1-\nu_e^2)} \tag{9}$$

where E_{PZT} represents the elastic modulus of the piezoelectric ceramic, ν_{PZT} represents the Poisson's ratio of the piezoelectric ceramic, h_{PZT} indicates the thickness of the monolithic piezoelectric ceramic, h_{copper} represents the thickness of the copper substrate, H represents the total thickness of the entire piezoelectric bimorph driver, h'_1 and h'_2 represent the thickness factor of the piezoelectric bimorphs:

$$\begin{cases} h'_1 = \dfrac{h_{PZT} + h_{copper}}{H} \\ h'_2 = \dfrac{h_{PZT}}{H} \end{cases} \tag{10}$$

E_e represents the equivalent elastic modulus after laminating of the single layer piezoelectric ceramic and copper substrate and ν_e represents the Poisson's ratio. The bending moment caused by the deformation of the dual-layer piezoelectric bimorph driven by the voltage U can be introduced by that from the single-layer piezoelectric bimorph. The bending moment under the action of the voltage U:

$$M_0 = D_e^{'} \frac{-2d_{31}U}{\frac{H}{2}+\frac{2}{H}\left(\frac{2}{E_{PZT}h_{PZT}}+\frac{1}{E_{copper}h_{copper}}\right)(2D_{PZT}+D_{copper})} \cdot \frac{1}{h_{PZT}} \tag{11}$$

where D_{PZT} represents the bending stiffness of a single piezoelectric ceramic, which can be calculated from:

$$D_{PZT} = \frac{E_{PZT}h_{PZT}^3}{12(1-\nu_{PZT}^2)} \tag{12}$$

D_{copper} represents the bending rigidity of the copper substrate, which can be calculated from:

$$D_{copper} = \frac{E_{copper}h_{copper}^3}{12(1-\nu_{copper}^2)} \tag{13}$$

and U is the driving voltage applied on the piezoelectric bimorphs.

4. Device Structures and Design

When the probe is immersed in the blood to be measured, the blood sample will also generate some resistance to the upper and lower vibrations of the probe. As the blood coagulation progresses, the resistance of the probe is gradually increased, and the amplitude of the electrical signal will gradually become smaller. The amplitude of the signal and the slope of the coagulation curve will reflect the blood clotting process. Generally speaking, a single piezoelectric ceramic chip cannot be directly used as a piezoelectric oscillator and the piezoelectric ceramic layer should be bonded with the metal substrate to form a bending vibration.

The substrate has three main functions. Firstly, the piezoelectric ceramic as a brittle material, is without high toughness, and easily broken by the additional force. Therefore, after bonding to the metal substrate, the mechanical properties of the whole system can be strengthened. Secondly, compared with other materials, the quality factor of the piezoelectric ceramic mechanical is low which leads to more energy consuming. Besides, a thicker piezoelectric ceramic chip requires greater voltage to maintain the vibration. However, the metal substrate will store elastic potential energy after the ceramic bonding in order to enhance the output capacity. In addition, the last metal substrate also plays a significant role in the displacement amplification. In this paper, we select and use the piezoelectric bimorphs shown in **Figure 2**, and the performance parameters are shown in **Table 1**.

Both the probe and the coupling joint are cylindrical rods. The probe sticks to the center of the lower piezoelectric bimorphs. The coupling joint is connected between the upper and lower piezoelectric bimorphs. The material of the probe and coupling joint is DSM Somos Imagine 8000 resin. DSM Somos Imagine 8000 resin has the advantages of small density, high processing precision, non-toxic harmless and little effect on blood coagulation. All of these advantages

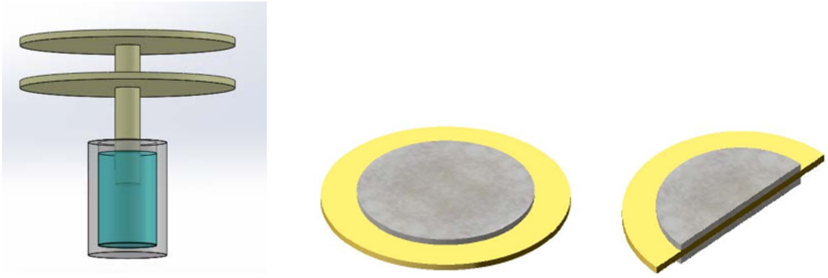

Figure 2. Schematic diagram of the detection device and 21 mm PZT bimorph.

Table 1. Performance parameters of piezoelectric bimorphs.

Parameter	Value	Parameter	Value
Maximum output voltage	30 V DC	Telescopic electromechanical coupling coefficient	0.43
Maximum output current	10 mA	Free permittivity	2000
Resonant impedance	<95 Ω	Mechanical quality factor	85
Static capacitance	81 - 91 nF	Plane electromechanical coupling coefficient	0.65
Copper thickness	0.18 mm	Kt33	2250
Piezoelectric ceramic thickness	0.10 mm	Piezoelectric ceramic material	PZT-5

with confirmed physical parameters facilitate the mathematic modeling and simulation analysis. The material parameters of the DSM Somos Imagine 8000 resin are shown in **Table 2**.

Since the piezoelectric ceramic layer is fixed to the metal substrate, the piezoelectric bimorphs can be fixed by the metal substrate. Therefore, this paper proposes the mechanical structure as shown in **Figure 3**. The upper part of the metal substrate is fixed and the liquid to be measured is placed into the lower base. The piezoelectric bimorphs are placed in the middle of the hollow slot. There is an embossed part of the metal substrate on the bottom of the upper part of the structure. The embossed part will suppress the edge. After the overall structure is fixed by the bolts of the two opposite sides, the metal substrate is also pressed. Therefore, the piezoelectric bimorphs are fixed well.

In order to ensure that the metal substrate is pressed, the height of the embossed part is slightly larger than the difference between the groove depth and the thickness of the metal substrate and the resulting height difference can be compensated by the gasket.

5. System Simulation

After setting the boundary condition, the initial value of the system and the load, the model is divided into the grid. The characteristic frequency option is selected in the research option, and the resonant frequency of 1 to 5 is selected in the order setting. Then we can obtain the vibration mode of the two-dimensional and three-dimensional drawing groups, which are shown in **Figures 4-8**.

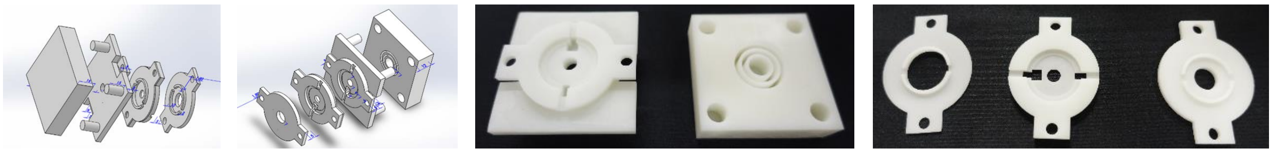

Figure 3. Mechanical structure and element.

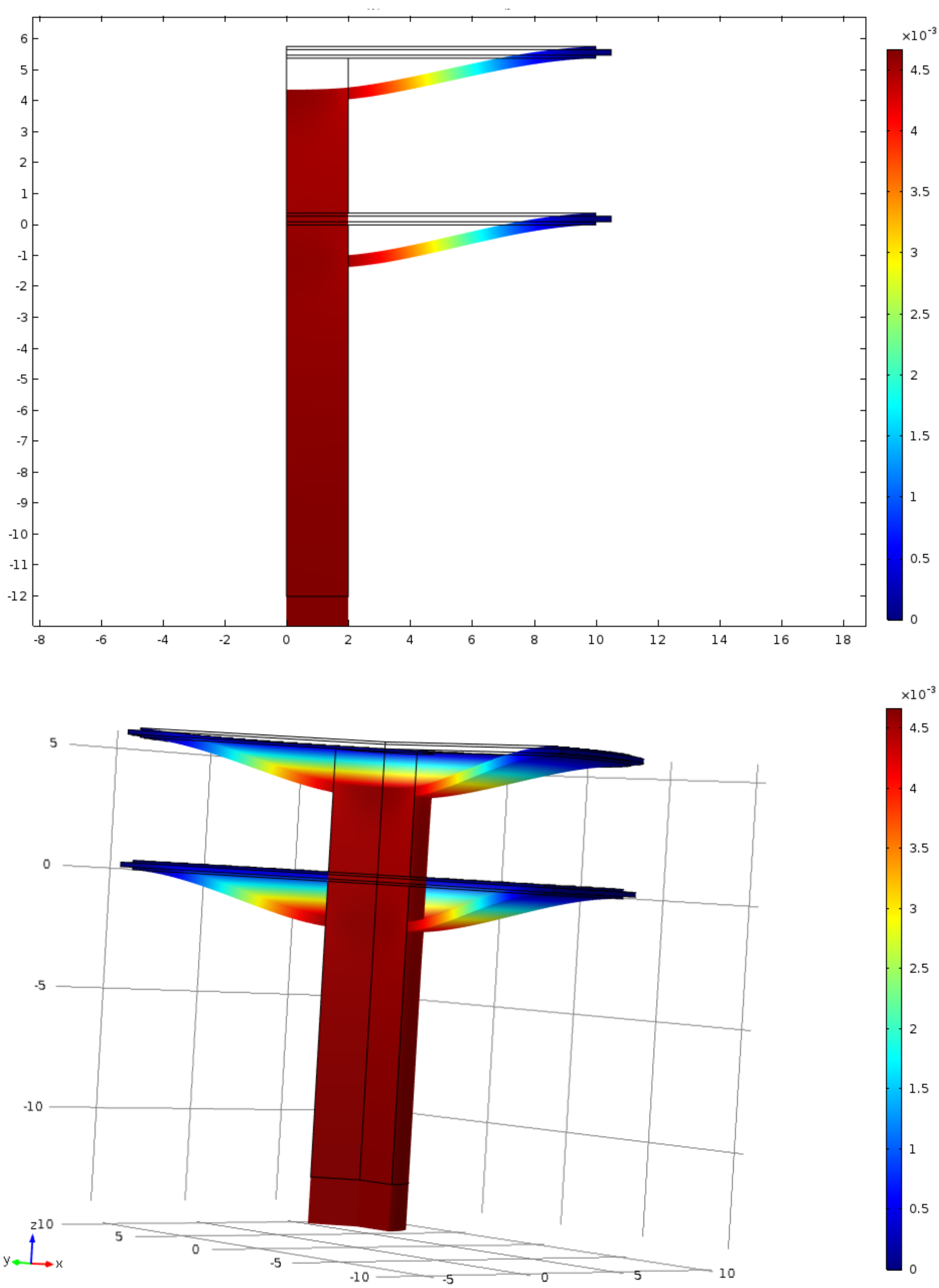

Figure 4. First-order mode.

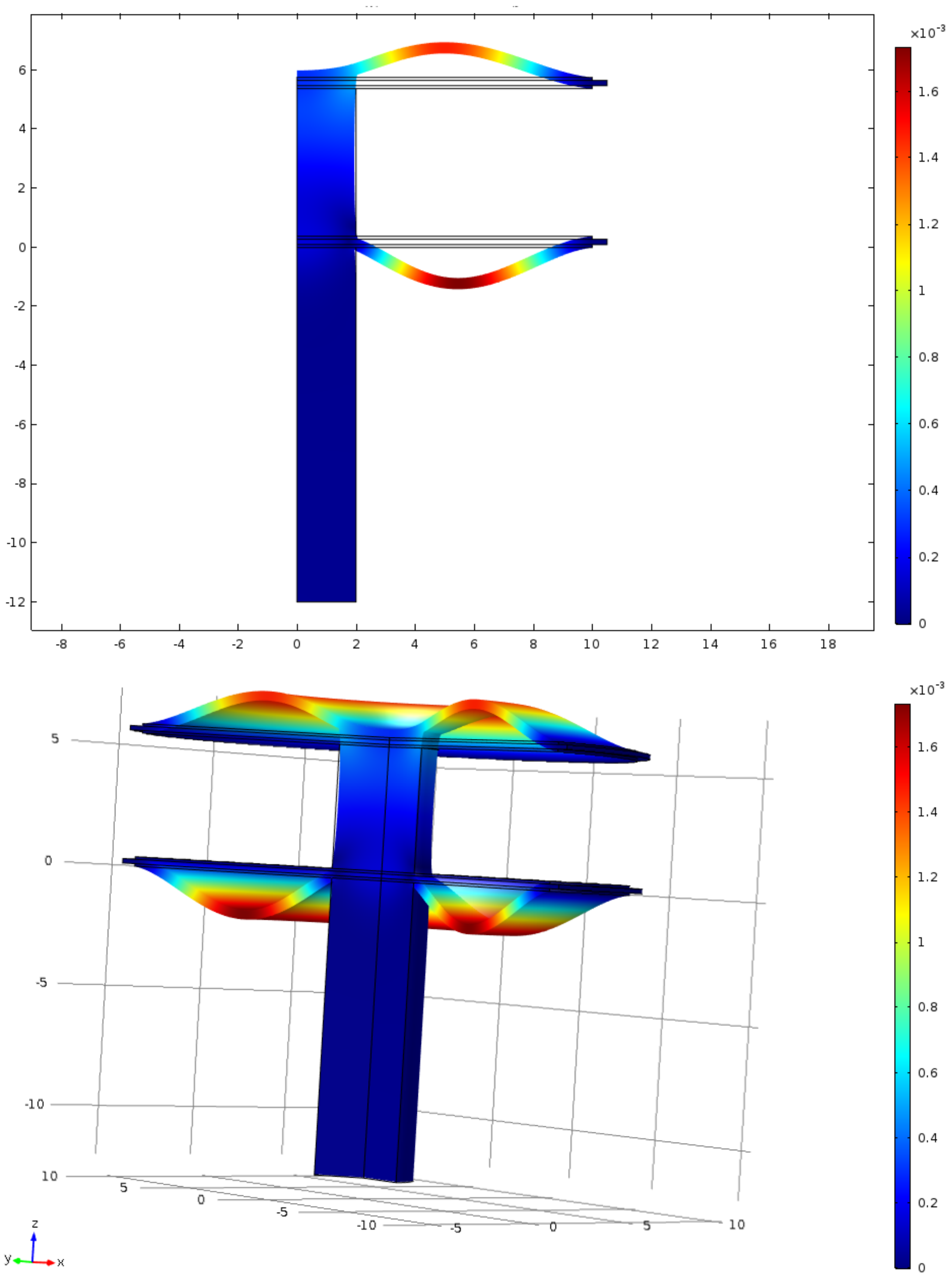

Figure 5. Second-order mode.

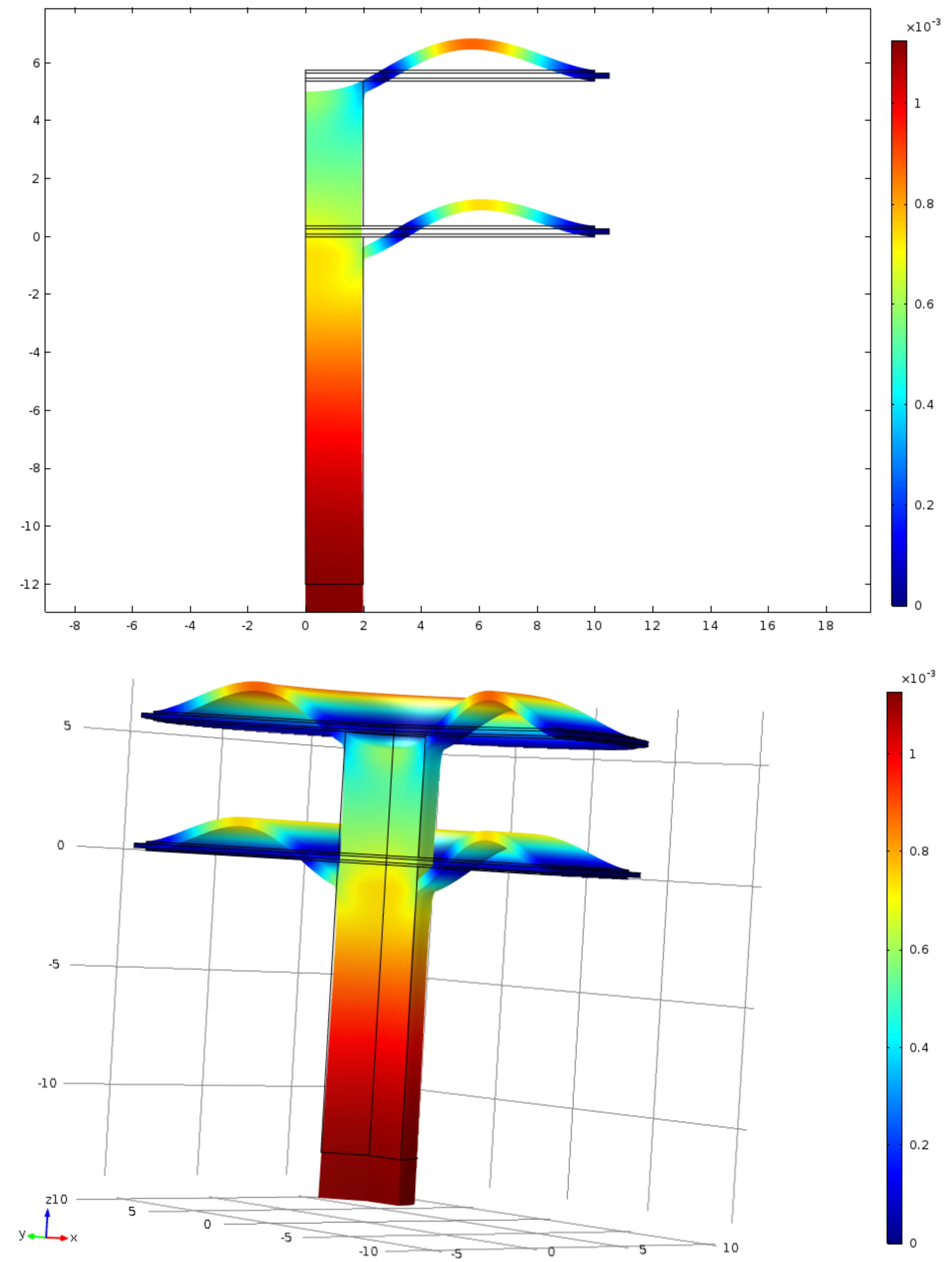

Figure 6. Third-order mode.

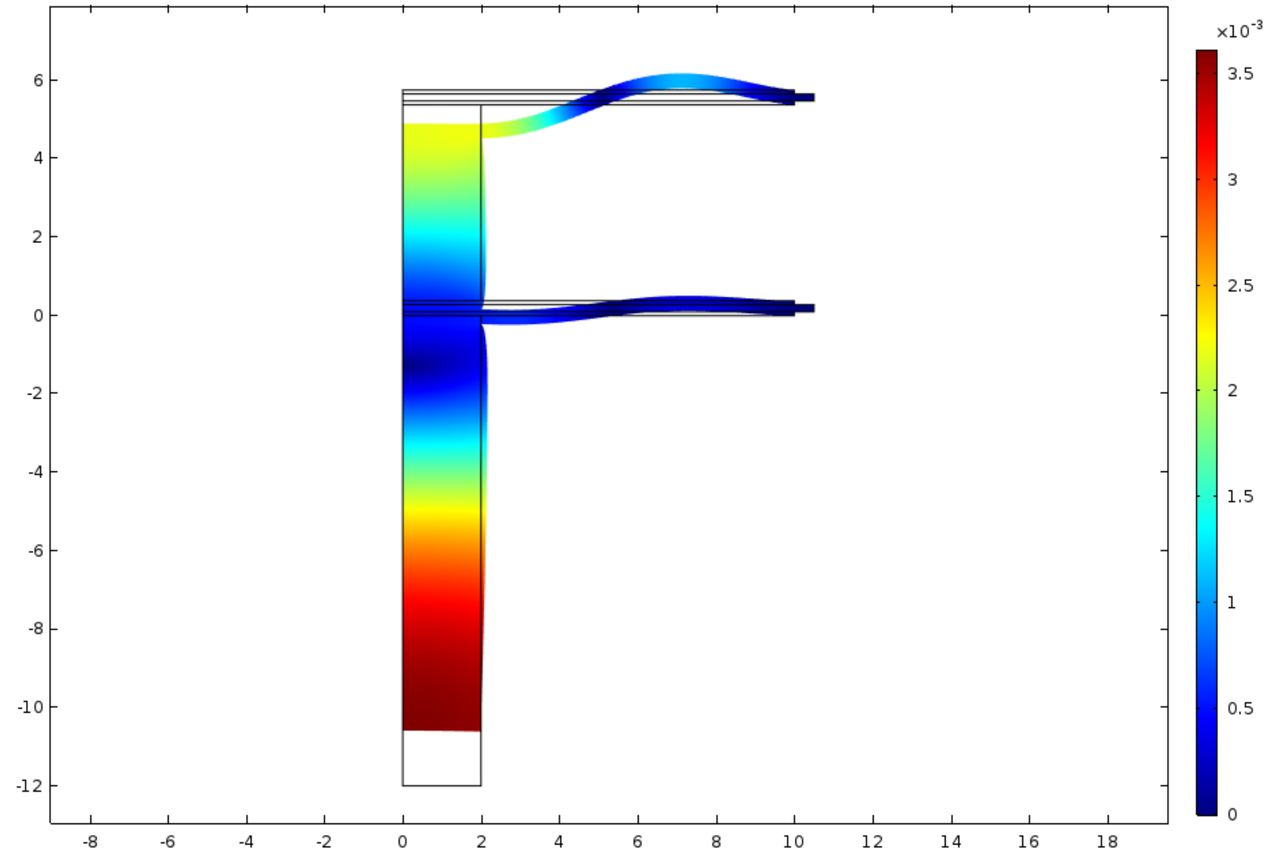

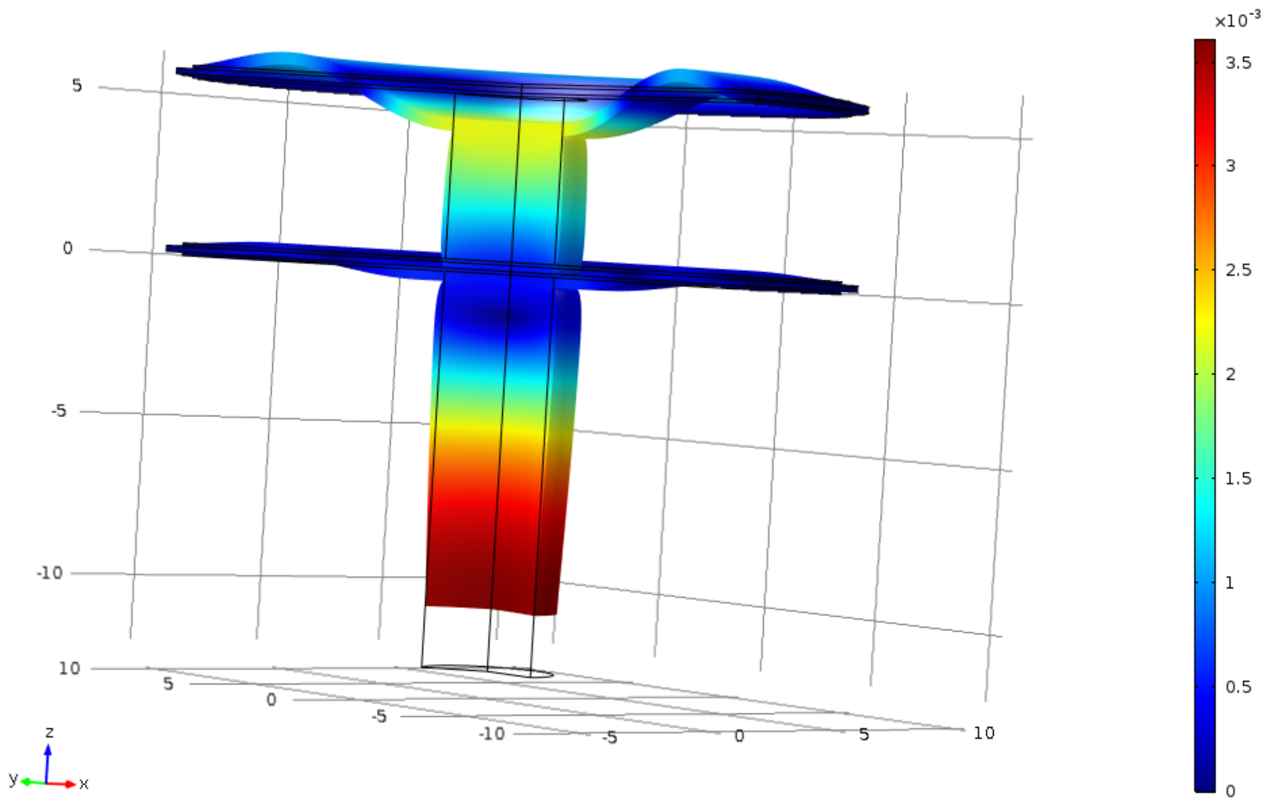

Figure 7. Fourth-order mode.

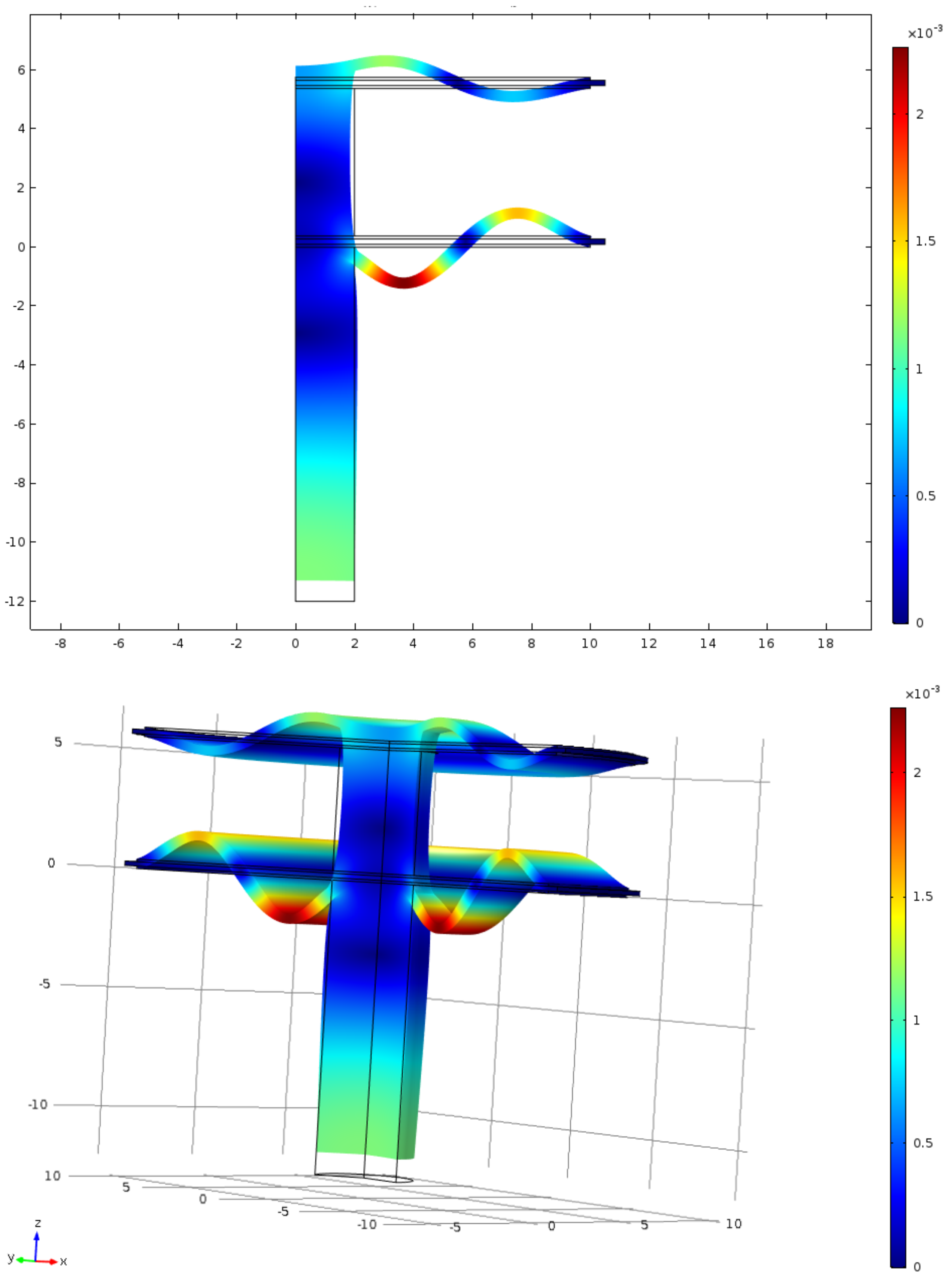

Figure 8. Fifth-order mode.

Table 2. Parameter of the DSM Somos imagine 8000 resin.

Parameter	Value
Viscosity	340 cps
Density	1.16 g/cm^3
Young's modulus	2510 Mpa
Tensile strength	37 Mpa
Elongation	7.5%
Poisson's ratio	0.41
Shore hardness	79
Yield elongation	3%
Dielectric constant	3.7
Flexural strength	67.3 Mpa
Flexural modulus	2200 Mpa

According to the simulation results, we can conclude that the first-order mode frequency is 4557 Hz. In the first-order vibration mode, the vibration of the center of the piezoelectric bimorphs is driven in the vertical direction. The second-order modal frequency is 15,217 Hz. In the second-order vibration mode, the edge and the center of the piezoelectric bimorphs are fixed. The annular part of the upper piezoelectric bimorphs is bent upward while the annular portion of the lower piezoelectric bimorphs is bent downward. Besides, the deformation of the probe and the coupling joint is not obvious. From the results of simulation analysis, we can also draw a conclusion that the third-order modal frequency is 18,633 Hz. In the third-order vibration mode, the two piezoelectric bimorphs have the same deformation. The edge and the center can be seen as two different nodes. The part between the center and the two nodes is distorted while the coupling joint deformation is not obvious. The probe deformation is in the vertical direction mainly. The fourth order modal frequency is 33,900 Hz. In the fourth order vibration mode, the deformation is similar to the third order vibration mode, but the deformation of the probe is mainly shortened.

In all modes of vibration, the first order mode is the ideal way to generate vertical vibrations. For other high order vibration modes, the deformation of piezoelectric bimorphs is more complex, the probe cannot form a stable and reliable vertical vibration. Therefore, we can set frequency of the drive voltage near the first order resonant frequency in order to get the ideal vibration. Moreover, we can conclude that in order to make the system frequency increase, it is useful to reduce the piezoelectric bimorphs radius, increase the coupling joint radius, reduce the length of the coupling connector, and reduce the radius and length of the probe. Among them, the change of the geometric dimension of the coupling joint and the probe geometry is similar, but there is no significant change in the radius of the piezoelectric bimorphs. And the other important index called as the maximum deformation is greater if the intrinsic frequency is smaller. The maximum the deformation is always at the scale of a few microns.

As can be seen from **Figure 9**, the displacement of the bottom of the structure reaches a maximum at 4550 Hz. Because of the first order of the intrinsic frequency, the system produces a resonance effect and a peak of the displacement. The average displacement of the bottom of the probe is at the scale of a few microns.

6. Experiments and Analysis

The probe is immersed into starch fluid and honey syrup that are two kinds of typical non-Newtonian fluids. The input sinusoidal signal is 5 Vpp, with the frequency gradually increasing from 10 Hz at the 1 Hz step.

The results are shown in **Figure 10** where the red curve represents the starch fluid and the green curve represents the honey syrup. As can be seen from **Figure 10**, the output voltage is greatly different from each other at the resonant frequency. However, at other frequencies, the difference is not very significant. Consequently, we may detect the viscoelasticity distinction among different non-Newtonian fluids at the resonant frequency.

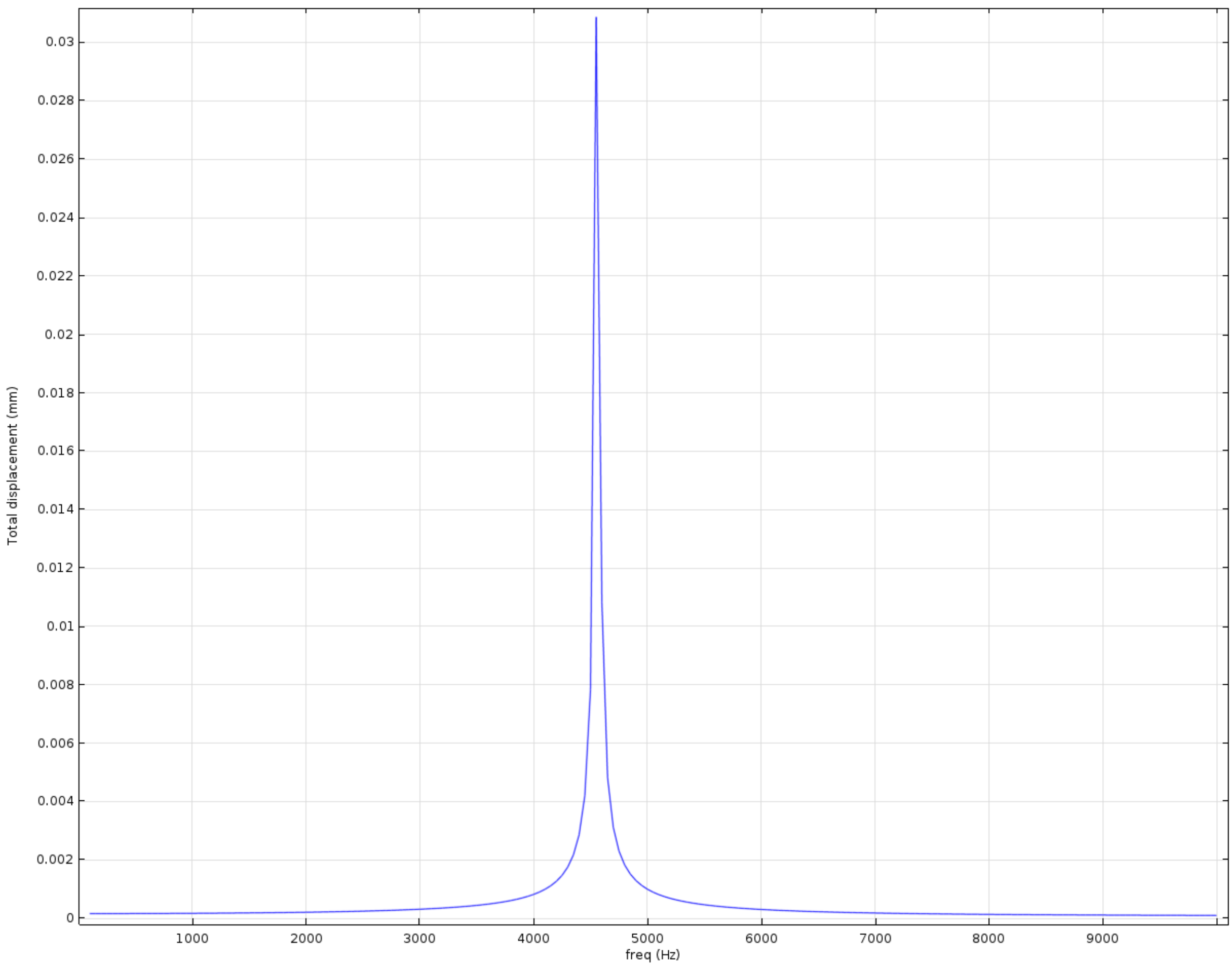

Figure 9. Average displacement-frequency curve at the bottom of the probe.

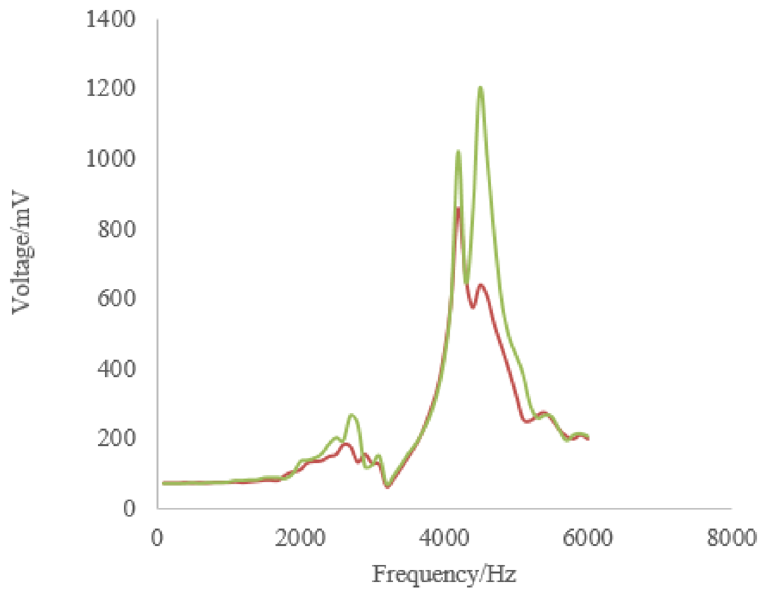

Figure 10. Comparison of output signals from starch fluid and honey syrup.

As is shown in **Figure 11**, we also measure the deformation using the Doppler vibration meter OFV-5000, which is a non-contact, ultra-precision laser vibration meter. The measurement results can be given from the near-DC to 24 MHz frequency range and the speed ranges up to ±10 m/s. The displacement range can be from one thousandth of a nanometer to meter. In the actual operation, the device will be placed on the air floating table and the laser will be aimed at the center of the piezoelectric bimorphs. After setting the range, resolution and other parameters, we can make the measurement results displayed on the oscilloscope as voltage values. Then the size of the displacement can be obtained by formula conversion. The input peak-to-peak voltage is 5 V sinusoidal signal and the frequency gradually increases to 7000 Hz from 10 Hz at the 5 Hz step size, the results shown in **Figure 12**.

Figure 12 shows the relationship between the deformation of the system and the frequency for starch fluid and honey syrup. When the frequency is near 4000 Hz, that is, the resonant frequency, the displacement and the output voltage have the exactly similar change trend. While at the 3000 Hz or so, the trend is similar, but the same displacement is corresponding to a much smaller output. Taking into account the simulation and the vibration analysis, the first order of the natural frequency will make the central portion of the piezoelectric bimorphs vibrate vertically. However, the other frequencies will make the piezoelectric bimorphs at the distorted vibrating states in some planes.

7. Conclusion

In this paper, a non-Newtonian fluid viscoelasticity measurement method based on piezoelectric effect is proposed. We use a piezoelectric bimorph with a diameter of 21 mm and a piezoelectric double crystal coupling driver with a DSM coupling probe with length of 3 mm, 5 mm and 7 mm. Several different non-Newtonian

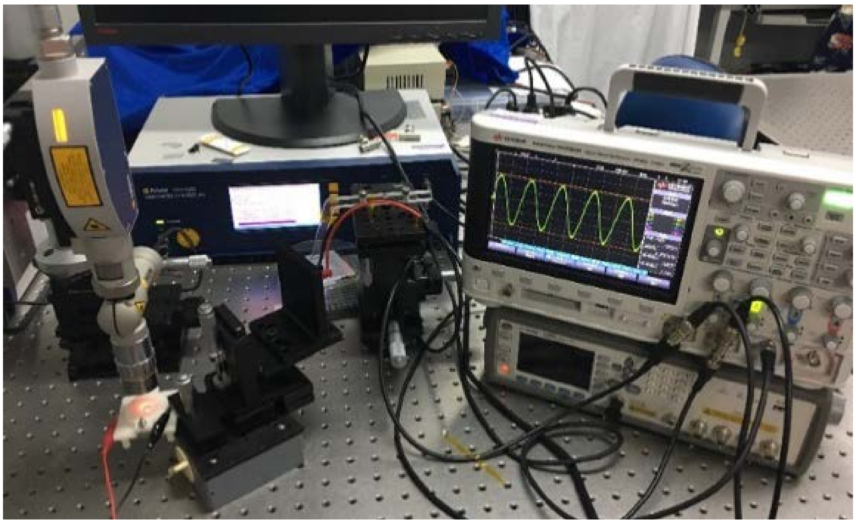

Figure 11. Vibration measurement of the piezoelectric bimorphs by OFV-5000.

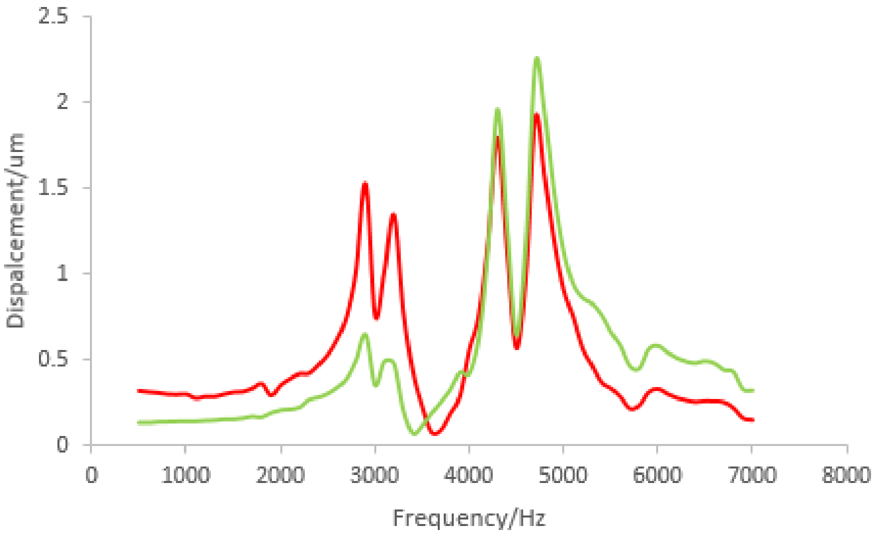

Figure 12. Relationship between the deformation of the system and the frequency.

fluid viscoelasticity were tested, and the vibrational amplitude of the piezoelectric and liquid surfaces was between 0.43 μm and 3.52 μm. When the frequency is near 4000 Hz, that is, the resonant frequency, the displacement and the output voltage have the exactly similar change trend. The feasibility of *in vitro* detection of thrombus was confirmed in principle, and the above scheme was validated by theory and experiment, which provided the basis for the measurement of blood viscoelasticity and the *in vitro* detection of thrombus and the engineering of the subsequent blood coagulation analyzer.

References

[1] Qari, M. (2005) High Throughput Coagulation Analyzers Review. *Combinatorial Chemistry & High Throughput Screening*, **8**, 353-360. https://doi.org/10.2174/1386207054020796

[2] Lippi, G., Favaloro, E.J., Franchini, M. and Guidi, G.C. (2009) Milestones and Perspectives in Coagulation and Hemostasis. *Seminars in Thrombosis and Hemostasis*, **35**, 9-22. https://doi.org/10.1055/s-0029-1214144

[3] Herbstreit, F., Winter, E., Peters, J. and Hartmann, M. (2010) Monitoring of Haemostasis in Liver Transplantation: Comparison of Laboratory Based and Point of Care Tests. *Anaesthesia*, **65**, 44-49. https://doi.org/10.1111/j.1365-2044.2009.06159.x

[4] Kitchen, D.P., Jennings, I., Kitchen, S., Woods, T.A. and Walker, I.D. (2015) Bridging the Gap between Point-of-Care Testing and Laboratory Testing in Hemostasis. *Seminars in Thrombosis and Hemostasis*, **41**, 272-278. https://doi.org/10.1055/s-0035-1544197

[5] Collet, J.-P., Shuman, H., Ledger, R.E., Lee, S. and Weisel, J.W. (2005) The Elasticity of an Individual Fibrin Fiber in a Clot. *Proceedings of the National Academy of Sciences of the United States of America*, **102**, 9133-9137. https://doi.org/10.1073/pnas.0504120102

[6] Seidel, H., Rahman, M. and Scharf, R. (2011) Monitoring of Antiplatelet Therapy. *Hämostaseologie*, **31**, 41-51. https://doi.org/10.5482/ha-1146

[7] Luddington, R. (2005) Thrombelastography/Thromboelastometry. *International Journal of Laboratory Hematology*, **27**, 81-90. https://doi.org/10.1111/j.1365-2257.2005.00681.x

[8] Tanaka, K.A., Szlam, F., Sun, H.Y., Taketomi, T. and Levy, J.H. (2007) Thrombin Generation Assay and Viscoelastic Coagulation Monitors Demonstrate Differences in the Mode of Thrombin Inhibition between Unfractionated Heparin and Bivalirudin. *Anesthesia & Analgesia*, **105**, 933-939. https://doi.org/10.1213/01.ane.0000278868.23814.3b

[9] Wanaka, K., Asada, R., Miyashita, K., Kaneko, M., Endo, H. and Yatomi, Y. (2015) Novel HIT Antibody Detection Method Using Sonoclot® Coagulation Analyzer. *Thrombosis Research*, **135**, 127-129. https://doi.org/10.1016/j.thromres.2014.10.024

[10] Evans, P.A., *et al.* (2008) Rheometry and Associated Techniques for Blood Coagulation Studies. *Medical Engineering & Physics*, **30**, 671-679. https://doi.org/10.1016/j.medengphy.2007.08.005

[11] Miyashita, T. and Kuro, M. (1998) Evaluation of Platelet Function by Sonoclot Analysis Compared with Other Hemostatic Variables in Cardiac Surgery. *Anesthesia & Analgesia*, **87**, 1228.

[12] Wan, P., Tong, H.S., Zhang, X.Q., Duan, P.K., Tang, Y.Q. and Su, L. (2014) Diagnosis of Overt Disseminated Intravascular Coagulation in Critically Ill Adults by Sonoclot Coagulation Analysis. *International Journal of Hematology*, **100**, 125-131. https://doi.org/10.1007/s12185-014-1601-3

[13] Brissaud, M., Ledren, S. and Gonnard, P. (2003) Modelling of a Cantilever Non-Symmetric Piezoelectric Bimorph. *Journal of Micromechanics & Microengineering*, **13**, 832. https://doi.org/10.1088/0960-1317/13/6/306

[14] Brissaud, M. (2004) Modelling of Non-Symmetric Piezoelectric Bimorphs. *Journal of Micromechanics & Microengineering*, **14**, 1507. https://doi.org/10.1088/0960-1317/14/11/011

[15] Wang, Q., Quek, S.T., Sun, C.T. and Liu, X. (2001) Analysis of Piezoelectric Coupled Circular Plate. *Smart Materials & Structures*, **10**, 229. https://doi.org/10.1088/0964-1726/10/2/308